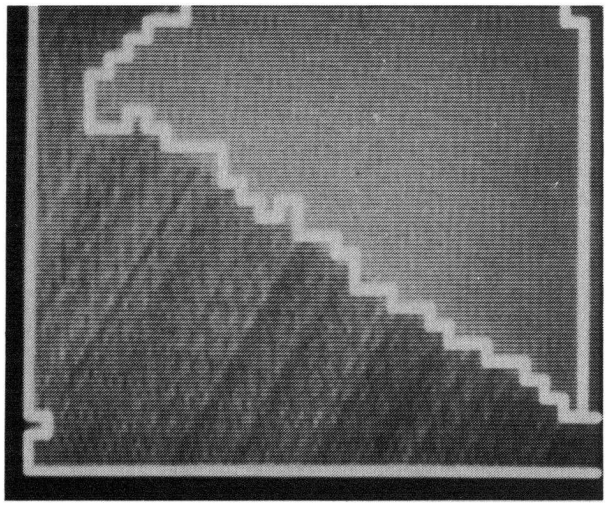

Fig. 9. Segmentation for Fig. 8.

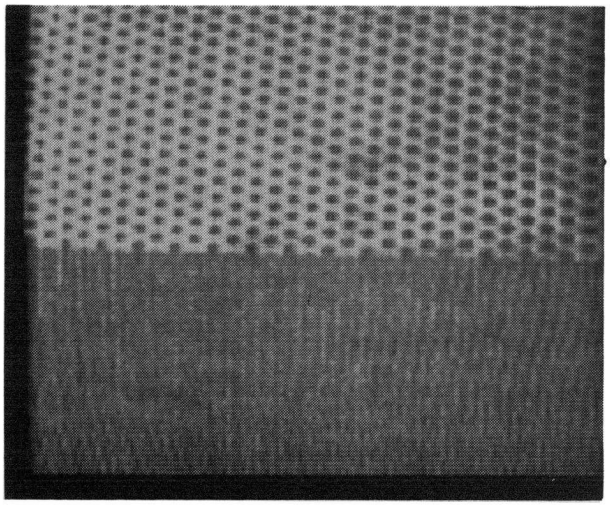

Fig. 10. Third picture with textures—one from a metal net and one from a carpet.

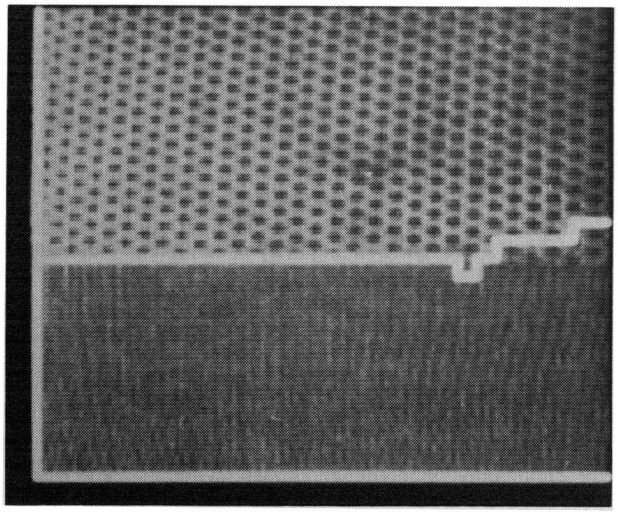

Fig. 11. Segmentation for Fig. 10.

it is 0.650, and for the group 3 it is 0.800. The final segmentations are shown in Figs. 7, 9, and 11.

VII. Conclusions

A second-order discrete Gaussian random field is proposed to model the texture. Based on the model, an approach which combines the statistical parameter estimation with the hierarchical segmentation scheme together is presented. The statistical method is used to analyze the spatial correlation of the texture and the hierarchical segmentation scheme is used to obtain the uniform region boundary. Only an approximate boundary can be found simply because the estimation accuracy decreases with the window size.

One basic assumption in this correspondence is that the numerical difference in the brightness function correspond to the perceptual differences. It is to be expected that regions of the image which appear similar would produce feature vectors that are near each other. However, this is not always the case. In addition to the fact that human perception of brightness is logarithmic, we have the problem that features which can be estimated mathematically may be difficult to perceive.

Acknowledgment

The authors would like to express their appreciation to Professor L. Wu of Fudan University, Shangai, for his valuable suggestions in the preparation of this correspondence.

References

[1] R. Haralick, "Statistical and structural approaches to texture," *Proc. IEEE*, vol. 67, pp. 786–804, May 1979.
[2] A. Rosenfeld and L. S. Davis, "Image segmentation and image model," *Proc. IEEE*, pp. 764–772, May 1979.
[3] G. B. Coleman and H. C. Andrews, "Image segmentation by clustering," *Proc. IEEE*, vol. 67, pp. 773–785, May 1979.
[4] T. Caelli and B. Julesz, "On perceptual analyzers underlying visual textural discrimination: Part I," *Biol. Cybern.*, vol. 28, pp. 167–175, 1978.
[5] T. Pavlidis, *Structural Pattern Recognition*. New York: Springer-Verlag, 1977.
[6] P. C. Chen and T. Pavlidis, "Image segmentation as an estimation problem," *CGIP*, vol. 12, pp. 153–172, Feb. 1980.
[7] S. L. Horowitz and T. Pavlidis, "Picture segmentation by a tree traversal algorithm," *JACM*, vol. 23, pp. 368–388, 1976.
[8] P. C. Chen and T. Pavlidis, "Segmentation by texture using correlation," Dep. EECS, Princeton Univ., Princeton, NJ, Tech. Rep. 265, May 1980.

On Edge Detection of X-Ray Images Using Fuzzy Sets

SANKAR K. PAL AND ROBERT A. KING

***Abstract*—The effectiveness of the theory of fuzzy sets in detecting different regional boundaries of X-ray images is demonstrated. The algorithm includes a prior enhancement of the contrast among the regions (having small change in gray levels) using the contrast intensifi-**

Manuscript received December 13, 1980; revised August 30, 1982. This work was supported in part by the Association of Commonwealth Universities in the United Kingdom and the Indian Statistical Institute, Calcutta, India.

S. K. Pal is with the Electronics and Communication Sciences Unit, Indian Statistical Institute, Calcutta, India on leave at the Department of Electrical Engineering, Imperial College of Science and Technology, London, England.

R. A. King is with the Department of Electrical Engineering, Imperial College of Science and Technology, London, England.

cation (INT) operation along with smoothing in the fuzzy property plane before detecting its edges. The property plane is extracted from the spatial domain using S, π and $(1 - \pi)$ functions and the fuzzifiers. Final edge detection is achieved using max or min operator. The system performance for different parameter conditions is illustrated by application to an image of a radiograph of the wrist.

Index Terms–**Contrast intensification, edge detection, enhancement, fuzzy set, image processing, S and π functions, X-ray.**

I. Introduction

The object of an edge detector is to detect the presence and location of changes in gray levels in an image. The methods so far developed for edge/contour detection of an image are categorized in two broad classes [1]–[5] namely, frequency-domain methods and spatial-domain methods. The technique in the first category is based on modification of Fourier transform of an image by a high-pass filter. The spatial-domain techniques on the other hand, are mostly based on the magnitude of discrete gradient corresponding to a pixel which measures the difference in intensity levels among the pixels. The edges are sharpened either by increasing the cutoff frequency of a high-pass filter (in frequency domain) or by using different threshold procedures (in spatial domain) [1], [2]. Because of the simplicity and yet effectiveness, the spatial domain techniques are mostly used in practical problems [2]–[5].

In X-ray processing problems, the appearance of an object on an X-ray film is a two-dimensional projection of a three-dimensional object. The film is therefore seen to contain a number of regions having fairly distinct gray levels (caused by variations of the transmission properties of tissue, cartilage, bone and multiple layers of bone) within the object superimposed on the background level. For example, in a radiograph of a hand and a wrist, these regions relate to small variations in grey level corresponding to soft tissue, single bone, superimposed bones, and palmar and dorsal surfaces [6] which have developed on the epiphysis of radius, ulna, phalanges, and metacarpal bones with the styloid process and other three-dimensional effects of bones due to the erroneous placing of the hand to be radiographed. The gray levels are minimum for background and maximum for palmar and dorsal surfaces. Since the change in gray level between these successive regions is not great and edge detection techniques are found to be effective only for significant contrast, it is necessary to enhance the contrast levels among the different regions of radiograph before detecting their regional boundaries.

The present work confines itself to demonstrating an application of the theory of fuzzy sets in the field of biomedical image processing for detecting contours of such regions on a radiograph of a hand and wrist. This is a part of the investigations of the research project "Identification of Skeletal Maturity and Adult Height from X-Ray," under development in the Digital Communication Section of the Electrical Engineering Department, Imperial College, London.

Since a gray tone image possesses some ambiguity within the pixels due to the possible multivalued levels of brightness, it is justified to apply the concept and logic of the fuzzy sets [7]–[9] rather than ordinary set theory to an image processing problem. Keeping this in mind, an image X can be considered as an array of fuzzy singletons [7]–[9], each with a membership function denoting the degree of membership of the singleton to X.

Fig. 1 presents the block diagram for detecting gray tone edges of an X-ray image using a fuzzy algorithm. This algorithm defines the edges in terms of the grade of membership function of the pixels with respect to some intensity level.

The procedure involves a pre-enhancement of an image by the stretching of its grey scale followed by a smoothing operation. These are done in block E_1. The smoothed image then

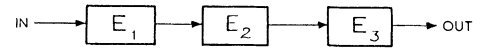

Fig. 1. Block diagram of the edge detection model.

undergoes a transformation (in block E_2) by G_W function (alternate use of π and $(1 - \pi)$ fuzzy functions) which results in contrast intensified k $(k > 3)$ regions of the X-ray image. The final edge detection is done in the block E_3 using "max" or "min" operator within neighbors or any other gradient technique [1], [2].

The technique used in the blocks E_1 and E_2 is based on modification of pixels in the fuzzy property plane of an image. This property plane is extracted from the spatial domain using S, π and their complement [7], [9] membership functions along with the fuzzifiers [9], [10]. The fuzzy contrast intensification (INT) operator is taken as a tool for enhancement in the property domain. Intermediate smoother is used for better primary enhancement.

The effectiveness of the algorithm with different values of the system parameters is demonstrated on an image of a wrist. The digital computer CDC 6400/6500/6600 was used as a processing system.

II. Fuzzy Set and Membership Function

A fuzzy set (A) with its finite number of supports $x_1, x_2, \cdots x_n$ in the universe of discourse U is defined as

$$A = \{(\mu_A(x_i), x_i)\} \tag{1a}$$

or, in union form

$$A = \bigcup_i \mu_i/x_i, \qquad i = 1, 2, \cdots, n \tag{1b}$$

where the membership function $\mu_A(x_i)$ having positive value in the interval (0, 1) denotes the degree to which an event x_i may be a member of A. This characteristic function can be viewed as a weighting coefficient which reflects the ambiguity (fuzziness) in A. A fuzzy singleton is a fuzzy set which has only one supporting point. If $\mu_A(x_i) = 0.5$, x_i is said to be the crossover point in A. The α-level set of A is defined as A_α, whose supporting points have membership value between α and 1, $0 < \alpha \leqslant 1$.

Similarly, the property p defined on an event x_i is a function $p(x_i)$ which can have values only in the interval (0, 1). A set of these functions which assigns the degree of possessing some property p by the event x_i constitutes what is called a propperty set (11).

A. Image Definition

With the concept of fuzzy set, an image X of $M \times N$ dimension and L levels can be considered as an array of fuzzy singletons, each with a value of membership function denoting the degree of having brightness relative to some brightness level l, $l = 0, 1, 2, \cdots L - 1$. In the notation of fuzzy set, we may therefore write,

$$X = \bigcup_m \bigcup_n p_{mn}/x_{mn} \tag{2}$$

$$m = 1, 2, \cdots, M; \qquad n = 1, 2, \cdots, N$$

where p_{mn}/x_{mn}, $(0 \leqslant p_{mn} \leqslant 1)$ represents the grade of possessing some property p_{mn} by the (m, n)th pixel intensity x_{mn}. This fuzzy property p_{mn} may be defined in a number of ways with respect to any brightness level depending on the problems at hand. In the following sections we will define the standard S and π fuzzy membership functions and their approximation in our problems.

B. S and π Functions and Property Plane

Two standard functions which are found in many cases to be convenient to represent the membership function of a fuzzy set in the real problems are the S and π functions. These are defined as [7], [9]

$$S(x; a, b, c) = 0, \quad x \leqslant a \tag{3a}$$

$$= 2\left(\frac{x-a}{c-a}\right)^2, \quad a \leqslant x \leqslant b \tag{3b}$$

$$= 1 - 2\left(\frac{x-c}{c-a}\right)^2, \quad b \leqslant x \leqslant c \tag{3c}$$

$$= 1, \quad x \geqslant c \tag{3d}$$

with

$$b = \frac{a+c}{2};$$

and

$$\pi(x; b, c) = S\left(x; c-b, c-\frac{b}{2}, c\right) \quad \text{for } x \leqslant c \tag{4a}$$

$$= 1 - S\left(x; c, c+\frac{b}{2}, c+b\right) \quad \text{for } x \geqslant c \tag{4b}$$

In $S(x; a, b, c)$, the parameter b is the crossover point, i.e., $S(b; a, b, c) = 0.5$. In $\pi(x; b, c)$, b is the bandwidth, i.e., the separation between the crossover points of π function, and c is the central point at which $\pi = 1$. Equations (3) and (4) define the membership or compatibility function corresponding to fuzzy sets "x is large" and "x is c" respectively.

Now in the case of the enhancement problem as discussed in Section III, one is ultimately interested in enhancing the contrast between successive adjacent regions (as needed for edge detection) by choosing only the crossover points, as the slope of the curves is not of interest. Therefore, we may approximate the functions S and π by $G(x_{mn})$ defined as [9], [10], [12].

$$p_{mn} = G(x_{mn}) = (1 + |\hat{x} - x_{mn}|/F_d)^{-F_e}. \tag{5}$$

Equation (5) represents in the interval $[0, x_{\max}]$, $x_{\max}$ being the maximum level in X, a membership function of S-type (G_S) for $\hat{x} = x_{\max} = L - 1$ corresponding to (3) over the range $a \leqslant x \leqslant c$. It represents, in the same interval, a π-type function (G_π) for $\hat{x}$ = some arbitrary level l_c, $0 < l_c < x_{\max}$ corresponding to (4) over the range $c - b \leqslant x \leqslant c + b$ with l_c corresponding to c.

The positive constants F_e and F_d [independent of (m, n)] are termed the exponential and denominational fuzzifiers, respectively. They have the effect of altering the ambiguity in the fuzzy property plane, and their values are determined automatically from the crossover points in the enhancement operation [12].

The function G_S represents, in the interval $[0, x_{\max}]$, the compatibility function corresponding to the fuzzy plane "x_{mn} is $x_{\max}$" and its fuzzy p_{mn} value denotes the degree of possessing maximum brightness level $x_{\max}$ by the (m, n)th pixel intensity x_{mn}. Similarly, G_π represents in the same interval, the compatibility function corresponding to the fuzzy plane "x_{mn} is l_c" and its p_{mn} value denotes the degree of possessing some arbitrary level l_c by the (m, n)th pixel.

The graphical representation of $p_{mn} = G_\pi(x_{mn})$ for different pixel intensities x_{mn} ranging from zero to $x_{\max}$ is shown in Fig. 2. Here l_1 and l_2 are the two crossover points, $(l_2 - l_1)$ is the bandwidth, and $l_c = (l_1 + l_2)/2 = x_{\max}/2$. The function is symmetric if $l_c = 2l_1$ or, alternatively, $l_c = 2l_2 - x_{\max}$. Otherwise, the function is nonsymmetric. For a G_S function, symmetry occurs when l_c [$= b$ in (3)] corresponds to $x_{\max}/2$ (middle of the range). Symmetry of the curve about the crossover points is controlled by the values of F_e and F_d.

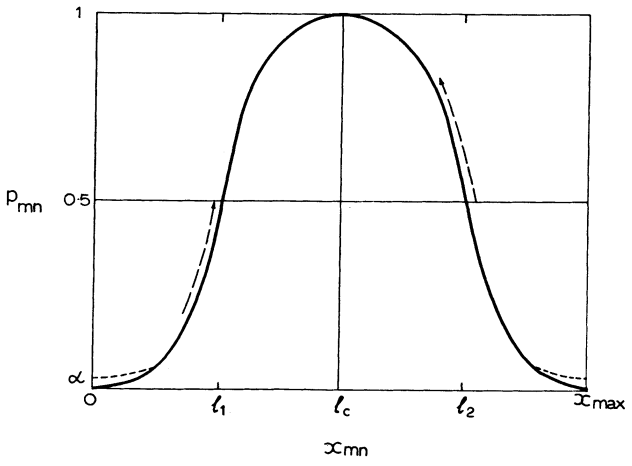

Fig. 2. π function for transforming x_{mn} to p_{mn}.

Therefore, instead of using two sets of piecewise nonlinear functions (3), (4) one can use (5) to represent S and π functions where the position of crossover points, bandwidth, and hence the symmetry of the curves are determined by the fuzzifiers F_e and F_d.

Again, it is to be noted from (5) that for $x_{mn} = 0$ or $2\hat{x}$, p_{mn} has a finite positive value α, where

$$\alpha = \left[1 + \frac{\hat{x}}{F_d}\right]^{-F_e}.$$

So the p_{mn} plane becomes restricted in the interval $(\alpha, 1)$ instead of $(0, 1)$ resulting in an α-level property plane of image X. This is shown in Fig. 2.

III. Enhancement of Contrast among Successive Regions

A. Contrast Intensification and Enhancement in Property Plane

The INT operator operating on a fuzzy set A generates another fuzzy set $A' = \text{INT}(A)$, the membership function of which is

$$\mu_{A'}(x) = \mu_{\text{INT}(A)}(x) = 2(\mu_A(x))^2, \quad 0 \leqslant \mu_A(x) \leqslant 0.5 \tag{6a}$$

$$= 1 - 2(1 - \mu_A(x))^2, \quad 0.5 \leqslant \mu_A(x) \leqslant 1. \tag{6b}$$

This operation reduces the fuzziness of a set A by increasing the values of $\mu_A(x)$ which are above 0.5 and decreasing those which are below it. Let us now define operation (6) by a transformation T_1 of the membership function $\mu(x)$.

In general, each p_{mn} in X (equation 2) may be modified to p'_{mn} to enhance the image X in the property domain by a transformation function T_r where

$$p'_{mn} = T_r(p_{mn}) = T'_r(p_{mn}), \quad 0 \leqslant p_{mn} \leqslant 0.5 \tag{7a}$$

$$= T''_r(p_{mn}), \quad 0.5 \leqslant p_{mn} \leqslant 1 \tag{7b}$$

$$r = 1, 2, \cdots.$$

The transformation function T_r is defined as successive application of T_1 by the recursive relationship

$$T_s(p_{mn}) = T_1\{T_{s-1}(p_{mn})\} \tag{8}$$

$$s = 1, 2, \cdots$$

and $T_1(p_{mn})$ represents the INT operator defined in (6).

The detail of the enhancement operation is reported in (12).

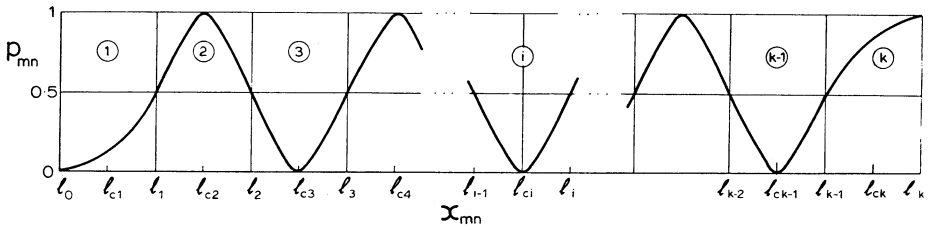

Fig. 3. G_W function; alternate use of π and $(1 - \pi)$ functions.

As r increases, the contrast between two/three consecutive regions corresponding to G_S/G_π will increase and in the limiting case, as $r \to \infty$, it will produce a two-tone (binary) image. For example, if we use the G_S function, the p'-values for the regions 0–l_1 and l_1–l_c would become zero and unity, respectively. Use of G_π, on the other hand, would result in unity property value for the region l_1–l_2 and zero for the rest (Fig. 2).

Thus, we see that by using suitable crossover points in S or π function it is possible to achieve any degree of contrast enhancement between two or three successive regions of gray levels in the p plane with an independent choice of r for T' and T'' operations.

B. Extension to Multiple Regions

Suppose we have more than three regions in the grey scale to be isolated from one another. The above concept can then be extended by the successive use of S or π functions over the regions in question. Fig. 3 shows such an alternate application of G_π and its complement $(1 - G_\pi)$ to enhance the contrast level among k regions $\Delta x_1, \Delta x_2, \cdots \Delta x_i, \cdots \Delta x_k$ ranging from l_0 to l_k in spatial domain.

Let $l_{c1}, l_{c2} \cdots l_{ci} \cdots l_{ck}$ denote the k central intensity levels of these regions, and $l_1, l_2 \cdots l_i, \cdots l_{k-1}$ are the intensities of the $(k - 1)$ boundary levels between these regions. Then we use

$$p_{mn} = G_W(x_{mn}) = G_\pi(x_{mn}; l_2 - l_1, l_{c2}), \quad x_{mn} \leqslant l_2 \tag{9a}$$

$$= 1 - G_\pi(x_{mn}; l_3 - l_2, l_{c3}), \quad l_2 \leqslant x_{mn} \leqslant l_3 \tag{9b}$$

$$\cdots$$

$$= 1 - G_\pi(x_{mn}; l_{k-1} - l_{k-2}, l_{c(k-1)}), \quad x_{mn} \geqslant l_{k-2} \tag{9c}$$

where

$$\Delta x_i = l_i - l_{i-1}; \; l_{ci} = \frac{l_i + l_{i-1}}{2}, \quad i = 1, 2, \cdots, k. \tag{10}$$

Since the central intensity points are obtained from the adjacent crossover points (10), the problem of separating k regions essentially reduces to the selection of $(k - 1)$ crossover points only. Again, in practice, each of the bandwidths Δx_i, $i = 1, 2, \cdots, k$ (although shown to be same in Fig. 3) is likely to be different.

If, after extracting the fuzzy properties using (9), we apply the T_r operation [(6)–(8)], the resulting modified $p'_{mn} \ll$ would contain k separable regions with a value of $p'_{mn} \ll 0.5/\gg 0.5$ corresponding to $\Delta x_i/\Delta x_{i+1}$, $i = 1, 2, \cdots$.

C. Inverse Membership Function

After the enhanced p'_{mn} domain is produced by $G_W(x_{mn}) \to T_r(p_{mn})$ transformation, we use

$$x'_{mn} = G_S^{-1}(p'_{mn})\Big|_{\substack{\hat{x}=x_{\max} \\ l_i=x_{\max}/2}}, \quad \alpha \leqslant p'_{mn} \leqslant 1 \tag{11}$$

to obtain the corresponding contrast intensified spatial domain x'_{mn}. Since the $G_S^{-1}(p'_{mn})$ yields a single valued (unlike G_π^{-1}) x'_{mn} domain whose dynamic range is determined by $\hat{x}$ and the symmetry about the crossover point is determined by F_e and F_d, the above transformation will generate a symmetrical spatial domain of full dynamic range (0 to $x_{\max}$). The resulting image X' would have valued either $x'_{mn} \gg x_{\max}/2$ or $\ll x_{\max}/2$ corresponding to $p'_{mn} \gg 0.5$ and $\ll 0.5$ in the alternate regions. The contrast (difference in grey level) between any two consecutive regions of X' would therefore approach $x_{\max}$.

D. Steps in the Processing Algorithm of Blocks E_1 and E_2

Steps in the processing algorithm encountered in blocks E_1 and E_2 of Fig. 1 are listed below where steps 1, 2, and 3 correspond to block E_1 and block E_2 comprises step 4.

1a) Extract the fuzzy properties of the image using a nonsymmetric G_S function (with crossover point corresponding to boundary level between the first two regions).

b) Apply the T'_r operator on the property plane to reduce the levels of first region only.

c) Apply the G_S^{-1} function [with the same parameters as in G_S of step 1a)] on the modified property plane to obtain the modified spatial domain.

2a) Extract the fuzzy property of image of step 1c) using a nonsymmetric G_S function (with crossover point corresponding to boundary level between last two regions).

b) Apply the T''_r operation on the property plane to enhance the levels of last region only.

c) Apply the G_S^{-1} function [with the same parameters as in G_S of step 2a)] on the modified property plane to obtain the modified spatial domain.

3) Smooth the image of 2c) in spatial domain to retrieve some pixel-intensities which have been greatly decreased/increased near the threshold in the T'_r/T''_r operations of steps 1 and 2.

4a) Extract the fuzzy properties of this smoothed image using the G_W function.

b) Apply the T_r operation on the property plane to enhance the contrast among successive regions.

c) Apply a symmetric G_S^{-1} function (with crossover point corresponding to $x_{\max}/2$) on the modified property plane to obtain the contrast-intensified successive regions in the spatial domain. The pixels of this domain are isolated by possessing gray levels either $\gg x_{\max}/2$ or $\ll x_{\max}/2$ in the alternate regions.

E. Implementation of Blocks E_1 and E_2

The block diagram of the enhancement process corresponding to step 1, 2, or 4 is shown in Fig. 4. The function $G(x_{mn})$ as defined by (5) uses two fuzzifiers F_e and F_d to extract the fuzzy properties p_{mn} for the (m, n)th pixel x_{mn} of an $M \times N$ input image X. The transformation function $T_r(p_{mn})$ serves the role of enhancement in the property plane using r successive applications of the fuzzy INT operator. This is explained by (6)–(8). The enhanced p' domain after being inversely transformed by $G^{-1}(p'_{mn})$ produces the corresponding enhanced image X' in the spatial domain.

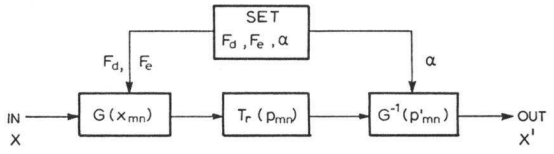

Fig. 4. Block diagram of the enhancement operation.

For steps 1 and 2, the function G corresponds to nonsymmetric G_S with different values of crossover points as determined by F_e and F_d. The crossover point in step 1 was allowed to fall at the boundary level of first two regions so that the operator T'_r can reduce the levels of the first region. The levels in other regions are unaffected. Similarly, the crossover point in step 2 was made to correspond to the boundary level of the last two regions so that the operator T''_r can only enhance the levels of last region without changing the others. In both cases, $\hat{x}$ was considered to be $x_{\max}$. The inverse function for these steps was G_S^{-1} with the parameters the same as in the respective G_S. For step 4, we used G_W, T_r (i.e., both T'_r and T''_r) and G_S^{-1} (symmetric across $x_{\max}/2$, $\hat{x} = x_{\max}$). The crossover points of these enhancement operations are chosen from the histogram of the images.

The smoothing operation in step 3 is achieved simply by an averaging technique within four neighbors such that the smoothed (m, n)th pixel intensity becomes

$$x'_{mn} = \frac{1}{4} \sum_{Q_1} x_{ij} \qquad (i, j) \neq (m, n), (i, j) \in Q_1. \tag{12}$$

Q_1 is a set of four neighboring coordinates which are on a circle of radius 1 unit from the point (m, n). After the smoothing operation, the sharp edges resulting from the application of thresholds in T' and T'' operations in steps 1 and 2 get blurred. This operation helps in getting back some parts of the picture lost (by T' operation in step 1) near the edges and also in selecting the final crossover points for the G_W function of step 4.

Again, since the p'_{mn}-values were obtained from the α-level property plane, it would contain some region where $p'_{mn} < \alpha$ due to the T'-operation. The algorithm thus includes a provision for constraining all the $p'_{mn} < \alpha$ values to α so that the above inverse transformation will allow those corresponding x'_{mn}-values to have zero gray level.

IV. Edge Detection

The edge detection using min or max operator [13] was adopted in block E_3 (Fig. 1) on the final enhanced spatial domain of 4c) (Section III-D). If x'_{mn} denotes the edge intensity corresponding to a pixel x_{mn}, then edges of the image are defined as

$$\text{Edges} \triangleq \bigcup_m \bigcup_n x'_{mn} \tag{13a}$$

where

$$x'_{mn} = |x_{mn} - \min_Q \{x_{ij}\}| \tag{13b}$$

or,

$$x'_{mn} = |x_{mn} - \max_Q \{x_{ij}\}| \tag{13c}$$

or,

$$x'_{mn} = \max_Q \{x_{ij}\} - \min_Q \{x_{ij}\}, \qquad (i, j) \in Q. \tag{13d}$$

Q is a set of N coordinates (i, j) which are on/within a circle of radius R centered at the point (m, n). Equation (13c) as compared with (13b) causes the boundary to be expanded by one pixel. Equation (13d), on the other hand, results in a boundary of two pixel width. It therefore appears from (13) that the better the contrast enhancement between the regions, the easier is the detection and the higher is the intensity of contours x'_{mn} among them.

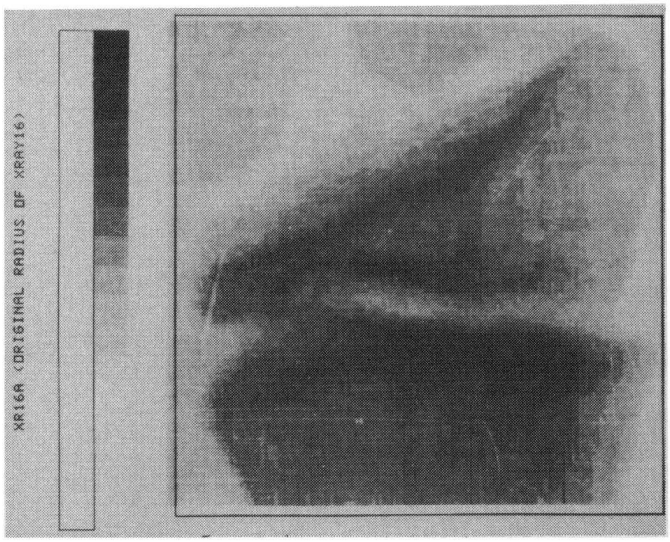

Fig. 5. Input image.

V. Experimental Results

Fig. 5 shows the radiograph of a part of the wrist containing a radius (with epiphysis and metaphysis) and a part of two small carpal bones taken from a boy in the age group of 10–12 years. The digitized version of the picture is represented by an array of 128×145 $(= M \times N)$ dimension having 256 $(= L)$ gray levels. The histogram of the image is shown in Fig. 6. It is seen from the histogram that the image contains 5 $(= k)$ regions approximating to 1) 50–80, 2) 80–100, 3) 100–135, 4) 135–165, and 5) 165–200. The first and the last regions correspond to soft tissue, and palmar and dorsal surfaces, respectively.

The first enhancement (step 1) has a crossover point of the nonsymmetric G_S function between 83 and 84, $F_e = 2$, and $\hat{x} = 255$ corresponding to $F_d = 414$ and $\alpha = 0.38296$ with $r = 4$. Step 2 has a crossover point of 166.5 (between 166 and 167), the same values of F_e, and $\hat{x}$ corresponding to $F_d = 213.6$, $\alpha = 0.2078$, and $r = 4$. After smoothing, the histogram is given in Fig. 7(a).

To compare the effects of a crossover point on the detection of palmar and dorsal surfaces, the values of F_d and α in step 2 above were changed to 223.3 and 0.21796 corresponding to a threshold level of 162.5; other parameters were unchanged. After smoothing, the changed histogram is as shown in Fig. 7(b). From Fig. 7(a) and (b) it is clear that the pixel intensities corresponding to the first region are reduced due to the T'_4 operation in step 1, thus making an extension of the region further down to the zero level. Similarly, the T''_4 operation in step 2 causes region 5 to extend further up to a level of 255 by increasing the pixel intensities belonging to that region. Since we are using the T'' operation, we need not bother about α in step 2. As an illustration of the smoothing operation, we have presented the smoothed image (Fig. 8) corresponding to Fig. 7(b).

In step 4, for Fig. 7(a) we have selected the values of l_1, l_2, l_3, and l_4 in the G_W function to be 55.5, 103.5, 138.5, and 163.5, respectively. For $F_e = 2$, the values of F_d corresponding to $l_{c1} = 79.5$, $l_{c2} = 121$, and $l_{c3} = 151$ were 58, 42.25, and 30, respectively. For Fig. 7(b), l_4 was changed to 159.5 (the other l_i's remaining the same) with a corresponding change in

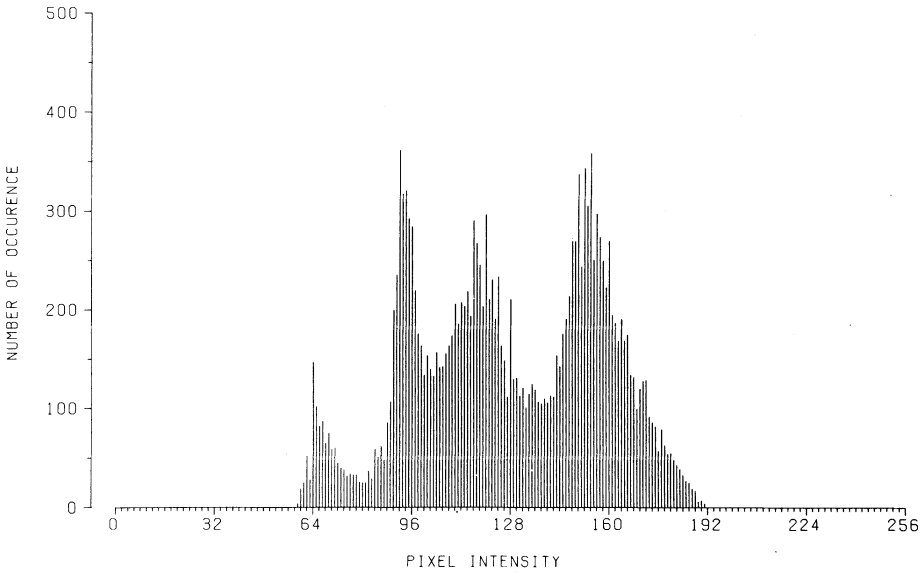

Fig. 6. Histogram of input image.

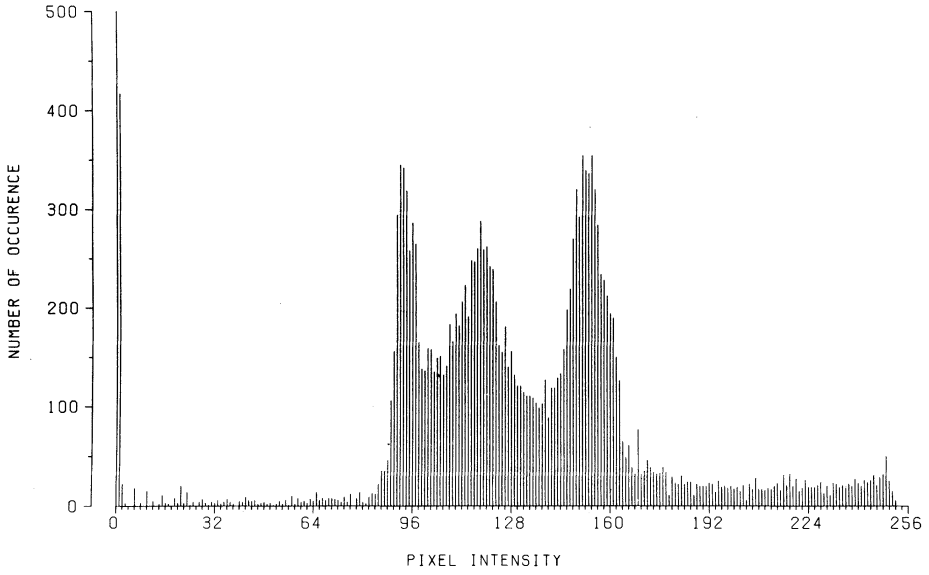

(a)

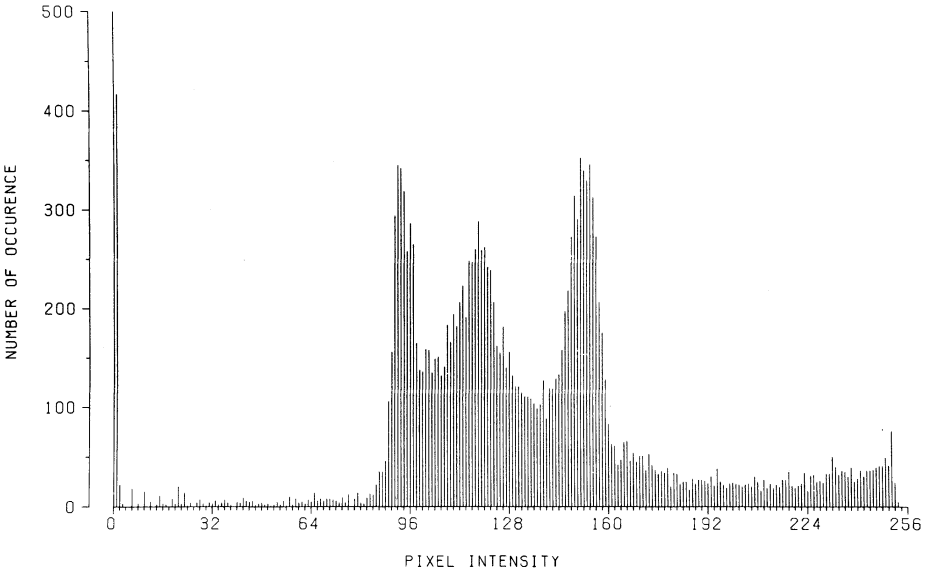

(b)

Fig. 7. Histogram of smoothed image. Crossover point in T_4'' operation corresponds to (a) 166.5, (b) 162.5.

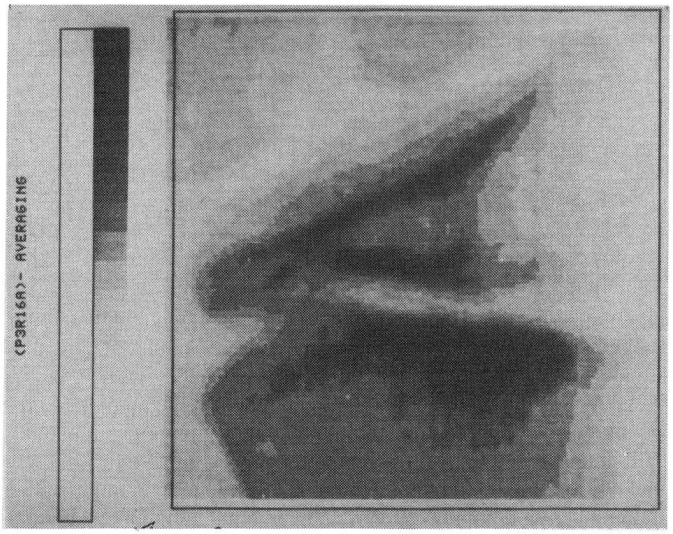

Fig. 8. Smoothed image corresponding to Fig. 7(b).

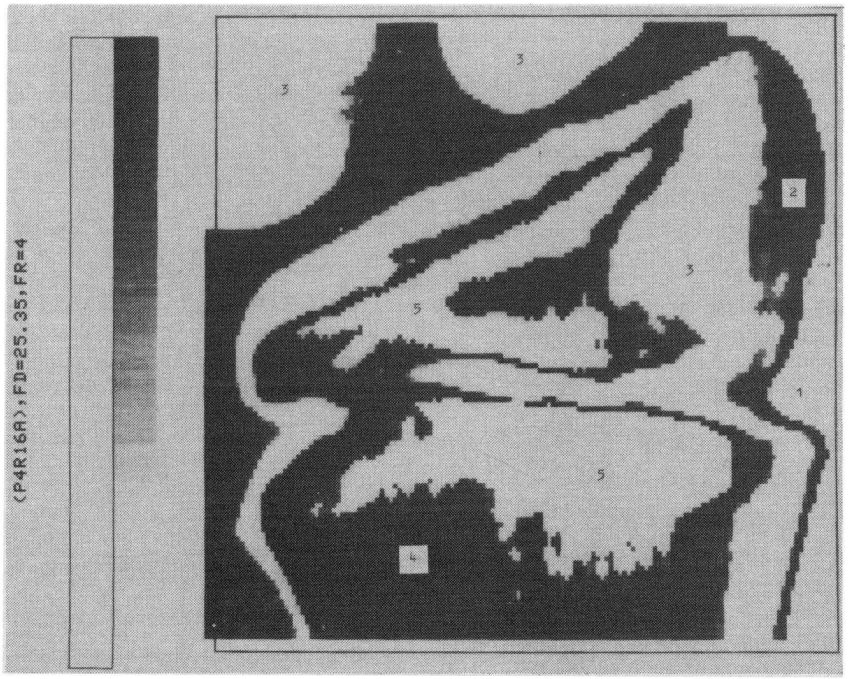

Fig. 9. Enhanced image showing isolation of five regions corresponding to Fig. 7(b) with $r = 4$.

F_d (= 25.35) and l_{c3} (= 149). T_4 was used here as an enhancement tool. For the symmetrical inverse transformation G_S^{-1}, we used $\hat{x} = 255$ and $F_d = 300$, $F_e = 2$ so that the crossover point becomes $\hat{x}/2$ and $\alpha = 0.2922$. The five contrast intensified regions of Fig. 8 as obtained after the fourth step (output of block E_2) of the algorithm is shown in Fig. 9.

Having completed the enhancement with blocks E_1 and E_2 we now consider edge detection in block E_3. The edge detection using min operator and $N = 4$, i.e., four neighbors (13b) is applied to images corresponding to Fig. 7(a) and (b), and the results are demonstrated in Fig. 10(a) and (b). Fig. 10(a) as compared to 10(b) is seen to lose some pixel intensities of palmar and dorsal surfaces.

If Fig. 8 is processed in block E_2 (step 4) by $r = 2$ or $r = 8$, and then edge detected as above with $N = 4$, we obtain Fig. 11(a) and (b), respectively. This demonstrates the effect of changing r in the INT operation. With changing r from $2 \rightarrow 4 \rightarrow 8$ [Fig. 11(a) $\rightarrow$ 10(b) $\rightarrow$ 11(b)] the image tends to become a two-tone (binary) and the detection of edges becomes better. The image obtained (in step 4) with $r = 8$ was also edge detected with $N = 5$ (including the (m, n)th point in min operation), but the result did not show any significant difference from Fig. 11(b). Fig. 12 shows the edges for $r = 8$ when (13c) ("max" operation) with $N = 4$ is used. The edges of Fig. 12 as compared to 11(b) are seen to be shifted by one pixel and it is the shift which makes the task of their interpretation more simplified as compared to Fig. 11(b) [15].

VIII. Conclusion

The concept of the fuzzy set and its associated operations are found to be applied successfully to the problems of gray tone image processing. The problem of detecting different regional contours of an X-ray film needs an initial enhancement of contrast among those regions before their detection. The use of fuzzy S and π functions along with the successive use of contrast intensifier is found to be suitable in isolating those regions in the property plane. The method is applicable for the images having distinctive peaks in their histograms. The crossover points and hence the placing of thresholds in enhancement operation are controlled by the fuzzifiers which

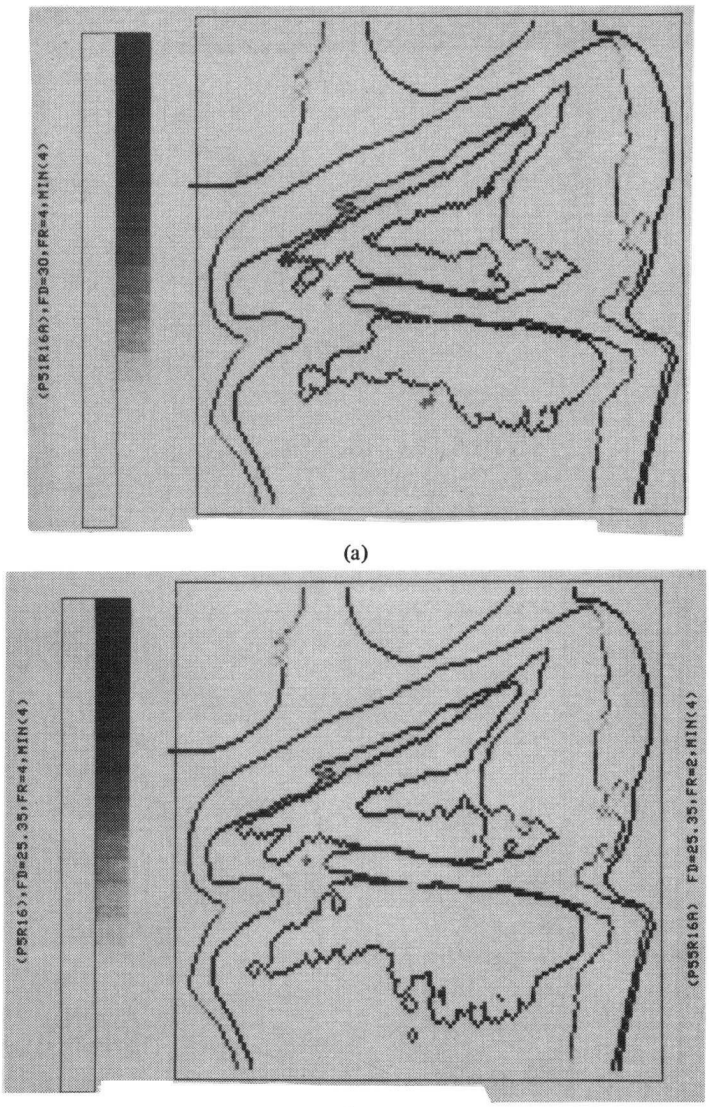

Fig. 10. Edge detected output using (13b) and $r = 4$. (a) Corresponding to Fig. 7(a), (b) corresponding to Fig. 7(b).

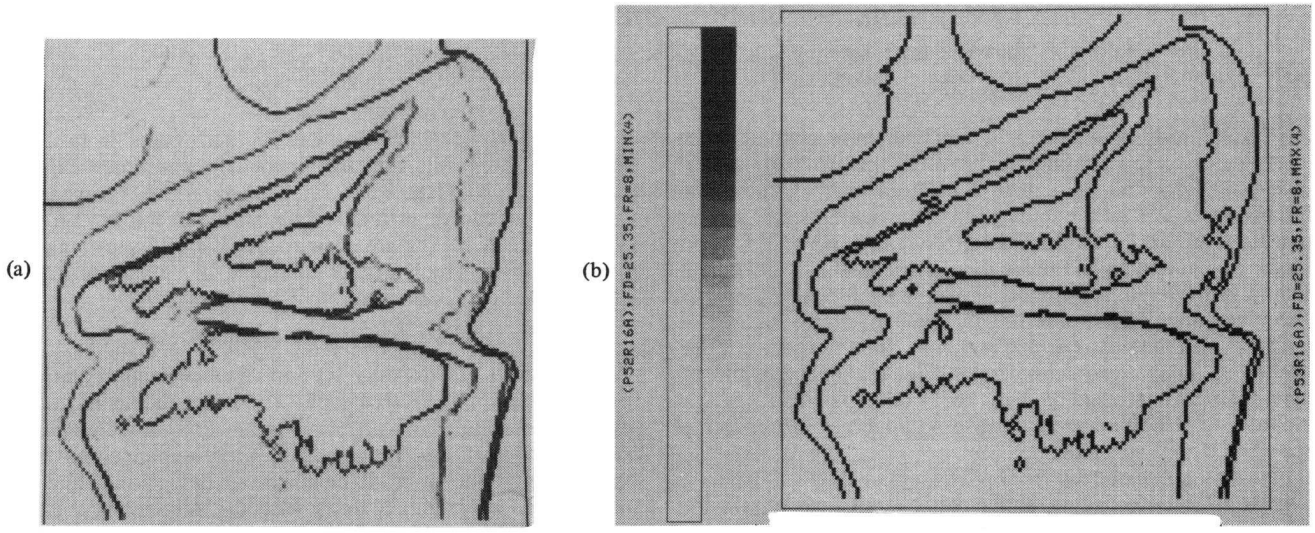

Fig. 11. Edge detected output using (13b) corresponding to Fig. 7(b). (a) $r = 2$, (b) $r = 8$.

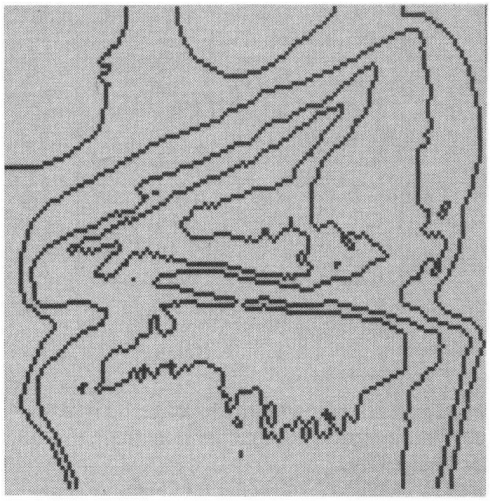

Fig. 12. Edge detected output using (13c) and $r = 8$ corresponding to Fig. 7(b).

play the role of creating different amounts of fuzziness in property domain. The intermediate smoother helps both in retrieving some pixel intensity lost by previous enhancement operations and in selecting the crossover points for the following final enhancement. Edge detection is done using min or max operators within the neighboring pixels. The edge intensity increases with the number of successive uses of the INT operator.

Investigations were also reported [14], [15] in which the preenhancement operation of block E_1 is replaced by the histogram equalization technique [2] (a standard existing enhancement operation for images like X-ray pictures and landscape photographs that are taken under poor illumination). But the contours of the resulting edge detected output image as compared to the present algorithm were seen to contain more spurious wiggles which, in turn, make the task of their description and interpretation more difficult.

ACKNOWLEDGMENT

Provision of X-ray films by Prof. J. M. Tanner is gratefully acknowledged by the authors. The authors' thanks are also due to Dr. A. A. Hashim for his valuable cooperation in this project.

REFERENCES

[1] A. Rosenfeld and A. C. Kak, *Digital Picture Processing*. New York: Academic, 1976.
[2] R. C. Gonzalez and P. Wintz, *Digital Image Processing*. London, England: Addison-Wesley, 1977.
[3] J. K. Agarwal, R. O. Duda, and A. Rosenfeld, Eds., *Computer Methods in Image Analysis*. New York: IEEE Press, 1977.
[4] *IEE Proc. Computer and Digital Techniques* (*Special Issue on Image Restoration and Enhancement*), vol. 127, p. 5, Sept. 1980.
[5] *IEEE Trans. Pattern Analysis Machine Intell.* (*Special Issue on Biomedical Pattern Analysis*), vol. PAMI-2, p. 5, Sept. 1980.
[6] J. M. Tanner, R. H. Whitehouse, W. A. Marshall, M. J. R. Healy, and H. Goldstein, *Assessment of Skeletal Maturity and Prediction of Adult Height* (*TW2 Methods*). New York: Academic, 1975.
[7] L. A. Zadeh, K. S. Fu, K. Tanaka, and M. Shimura, Eds., *Fuzzy Sets and Their Applications to Cognitive and Decision Processes*. London: Academic, 1975.
[8] P. P. Wang and S. K. Chang, Eds., *Fuzzy Sets–Theory and Applications to Policy Analysis and Information Systems*. New York: Plenum, 1980.
[9] S. K. Pal, "Studies on the application of fuzzy set theoretic approach in some problems of pattern recognition and man–machine communication by voice," Ph.D. dissertation, Calcutta Univ., Calcutta, India, 1978.
[10] S. K. Pal and D. Dutta Majumder, "Fuzzy sets and decision making approaches in vowel and speaker recognition," *IEEE Trans. Syst., Man, Cybern.*, vol. SMC-7, pp. 625–629, Aug. 1977.
[11] A. D. Allen, "Measuring the empirical properties of sets," *IEEE Trans. Syst., Man, Cybern.*, vol. SMC-4, pp. 66–73, Jan. 1974.
[12] S. K. Pal and R. A. King, "Image enhancement using smoothing with fuzzy sets," *IEEE Trans. Syst., Man, Cybern.*, vol. SMC-11, pp. 494–501, July 1981.
[13] Y. Nakagawa and A. Rosenfeld, "A Note on the use of local min and max operations in digital picture processing," *IEEE Trans. Syst., Man, Cybern.*, vol. SMC-8, pp. 632–635, Aug. 1978.
[14] S. K. Pal and R. A. King, "Histogram equalization with S and π functions in detecting X-ray edges," *Electron. Lett.*, vol. 17, pp. 302–304, Apr. 16, 1981.
[15] S. K. Pal, "Fuzzy set theory in grey tone image processing," Ph.D./D.I.C. dissertation, Imperial College, University of London, London, England, 1982.

Optimal Quadtrees for Image Segments

WILLIAM I. GROSKY AND RAMESH JAIN

Abstract–**Quadtrees are compact hierarchical representations of images. In this paper, we define the efficiency of quadtrees in representing image segments and derive the relationship between the size of the enclosing rectangle of an image segment and its optimal quadtree. We show that if an image segment has an enclosing rectangle having sides of lengths x and y, such that $2^{N-1} \times \max(x, y) \leq 2^N$, then the optimal quadtree may be the one representing an image of size $2^N \times 2^N$ or $2^{N+1} \times 2^{N+1}$. It is shown that in some situations the quadtree corresponding to the larger image has fewer nodes. Also, some necessary conditions are derived to identify segments for which the larger image size results in a quadtree which is no more expensive than the quadtree for the smaller image size.**

Index Terms–**Blueprint, grid size, image translation, optimal quadtree, partial quadtree.**

I. INTRODUCTION

Quadtrees are receiving increasing attention from researchers in computer graphics, image processing, cartography, and related fields. The quadtree representation of a region is based on successive subdivisions of the array into quadrants. A uniform quadrant of the image is represented by a leaf in the tree; a nonuniform quadrant is represented by an internal node, preparatory to its being further divided into its quadrants. Thus, the entire array is represented by the root node, the four quadrants by the four sons of the root node. This process is iterated. The leaf nodes, being of uniform color, represent those blocks for which no further subdivision is required. As an example, the 8×8 region shown in Fig. 1 is represented by the quadtree exhibited in Fig. 2; a white region is represented by a white node □; and a black region is represented by a black node ●. Note that the coordinate system we are using has the origin at the northwest corner, and that the positive

Manuscript received July 22, 1981; revised August 9, 1982.

W. I. Grosky is with the Intelligent Systems Laboratory, Department of Computer Science, Wayne State University, Detroit, MI 48202.

R. Jain was with the Intelligent Systems Laboratory, Department of Computer Science, Wayne State University, Detroit, MI 48202. He is now with the Department of Electrical and Computer Engineering, University of Michigan, Ann Arbor, MI 48109.